Bat-inspired Metaheuristic Convolutional Neural Network Algorithms for CAD-based Lung Cancer Prediction

P. Priyadharshini[1*] and B. S. E. Zoraida[1]

[1] *Department of Computer Science and Engineering, Bharathidasan University, Tiruchirappalli, India.*
[*] *Corresponding author. E-mail: Priyadimeet95@gmail.com*

Received: June. 02, 2020; Accepted: July. 01, 2020

In this real-world, lung cancer (LC) is the foremost reason for mortality in both mankind in the present time, with an inspiring figure of around five million deaths every year. Computer tomography (CT) can deliver valuable information when diagnosing lung illnesses. The chief goal of this work is to identify cancer nodules in the lungs from a given input image of the lungs and to organize LC and its harshness. To locate cancer nodules in the lungs, Fuzzy c-means (FCM) based segmentation is used. In this paper, a BAT optimization-based learning rate modified Convolutional Neural Network algorithm is introduced to effectively predict lung cancer. Additionally, to improve the proposed classification performance, input image is decomposed with support of the Discrete Wavelet Transform (DWT). With is used to decompose the image into four sub-bands, in such case we considered the Low (LL) band image. And then segmented images are split into two groups of images, which are used for the training and testing process. the proposed scheme has validated with the help of the LIDC-IDRI publically available dataset. They are studied by applying a convolutional neural network, and instantly trained neural network for predicting LC. In the end, the system efficiency is checked by using MATLAB tool to obtain the results of this model. In this experimentation, we achieved the accuracy of 97.43 % with a minimum classification error of 2.57 % in lung cancer prediction. This method is used to diagnose lung cancer correctly, and also this method may also overcome the previous drawbacks in the lung cancer diagnosis method.

Keywords: Fuzzy c-means (FCM), Computer Tomography (CT), Convolutional Neural Network (CNN), BAT optimization algorithm, Discrete Wavelet Transform, and LC Prediction.

http://dx.doi.org/10.6180/jase.202102_24(1).0008

1. Introduction

LC is one of the peak level types of cancer in the world. There are so many people are died due to lung cancer diseases [1], which accounts for around 19 % of cancer deaths. LC causes over 1.59 million deaths annually, prostate, and lung cancer per year [2]. Direct tobacco consumption accounts for more than 6.1 million deaths, and around 900,000 deaths are due to coverage to secondhand smoke [3]. The escalation in the LC rate joint with the nature of the relapse becomes a serious public health problem. Therefore, the need for a solution that can contribute to early detection is paramount. The increase in survival was slow in LC compared to most cancers [4], which means that the survival rate for LC is only 10 %. The National Lung Screening Study (NLST) in its echo, shows how helical CT can assist in decreasing LC death by 20 % [5]. Numerous scans have led to an upsurge in the sum of high-resolution computer tomography. In clinical practice, CT can detect fine granularity of the pulmonary nodules. Due to the high sensitivity of CT, extensive data are generated with complex uncertainty [6]. Therefore, it is difficult for radiologists to distinguish injuries from fit tissues. With the development of automation and data processing, the CAD method has shown greatly probable for diagnostic support. Segmentation is used to highlight a node in CT, while classification is used to determine if a node is malicious or empty.

The method has its drawbacks due to the discrepancy existing in the pulmonary nodes. Some of the related works analyzed, such as the author [7], used CNN technique to predict lung nodules from CT scan imagery. This system offers accuracy up to 84.32 %. After discussions among various authors, computer tomograms are inspected using segmentation and an optimized machine learning procedure to accurately predict cancer. And also, [8] has classified the normal structure of the lung analysis. Optimal retention is used for segmentation. Features are mined using geometric, statistical, and gray scale features. Latent Dirichlet allocation (LDA) is used for classification. The outcomes display 84 % accuracy, a sensitivity of 97.14 %, and a specificity of 53.33 %. Further increase the outcomes by the [9] has a projected procedure for detecting LC using a morphological operation to segment a region of interest in the lung from which a feature is extracted and used to classify cancer using an artificial neural network (ANN), the results show an accuracy of 92 %. It is better than the previous technique.

Further [10] has classified the cancer nodes by using SVM techniques. The input image was segmented using watershed segmentation. The characters are then mined using the area, eccentricity, center of gravity, diameter and average pixel intensity for segmented tumor nodes. After improving the differentiation of the gray scale picture, [11] has set up an LC knob discovery framework utilizing a fluffy induction strategy for grouping. The subsequent duplicate is portioned utilizing a functioning circle model. Highlights, for example, region, relationship, significant hub length, and minor hub length, are distant to make the classifier. The precision of the model [12] is 94.12 %. There are more noise present in the images, so that noise can be removed has used a Super-pixel segmentation and a Gabor filter. The first one is used for segmentation, and the Gabor filter is used to suppress noise in medical images. In general, the accuracy of the system is 89.5 %. In this article, we can change another classification algorithm to recognize an image of a cancer-prone area. In the above, we discussed some important techniques are presented by existing authors for lung cancer prediction techniques, in this discussion aids to find out the major problematic issues in LC detection and prediction process. The following difficulties are the learning rate is a hyper-parameter that controls how much the model should change in response to the error that is calculated each time the model weight is updated [13].

The stochastic gradient descent is simple to implement with many training patterns and is also quick in the event. However, the Conjugate gradient (CG) is slow and requires multiple processors and a lot of RAM. [14]. Hessian optimization was used to train deep auto-encoders [15] that have experience in solving the adjustment difficult and are more effective than the pre-training + fine-tuning projected by Hinton and Salakhut [16]. In fact, optimization methods are heuristic or counter-heuristic. These optimization methods were used to solve optimization difficulties in the research, technology, and even industry [17]. However, heuristic studies to optimize the deep learning process are rarely carried out. To overcome this existing problem, in this paper, we introduced the BAT algorithm used in both segmentation and classification processes to exactly diagnose lung cancer early.

2. Proposed Bat-inspired meta-heuristic CNN Algorithms

In this article, we match the presentation of three meta-heuristic algorithms to optimize CNN, such as Differential Evolution (DE), simulated annealing (SA), and Harmony Search (HS). The strategy is to find the finest value of the fitness function learning rate's using the meta-heuristic procedure. In addition, three different kinds of Optimization Algorithms are used to find the learning rate. The Optimization Algorithms such as PSO, ACO, and BAT. These three optimizations are combined with CNN algorithm for classification process to evaluate the classification accuracy. In the case of testing the presentation of the projected approaches, we use the LIDC-IBRI dataset. To improve the segmentation performance in this work, the FCM Algorithm is used. Finally, BAT optimization algorithm is combined with CNN to gain better classification performance. The basic flow drawing of the projected scheme is defined in Fig. 1.

2.1. LIDC-IBRI dataset

Lung Image Database dataset (LIDC-IDRI) comprises affectionate screening CT scans and LC with improved declared injuries. This is a universal resource that is open to PC improvement, preparation, and evaluation and has helped demonstrate CAD strategies for the prediction and detection of malignant lung neoplasms. Seven research centers and eight restorative visualization administrations worked together to create this compilation of 1018 cases. All subjects combine imagery from a clinical CT scan of the lungs and the corresponding XML archive. The possible results of the two-meter method for visual assessment are recorded by four experienced chest radiologists. In the proposed system, 200 images are trained in the LIDC-IBRI dataset, and 80 images are tested. Some of the sample record imagery are defined in Fig. 2.

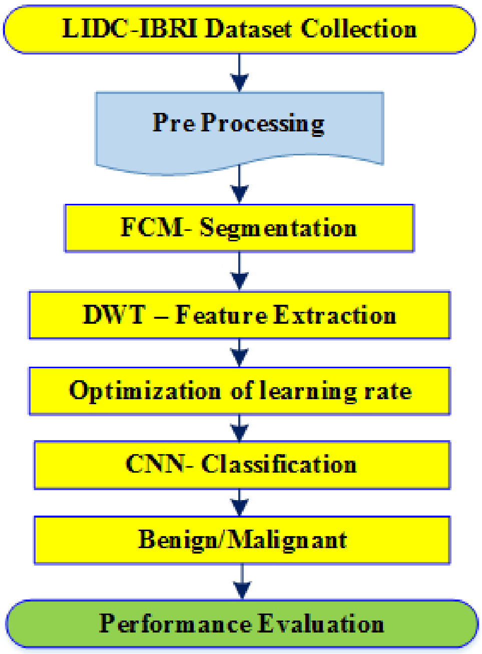

Fig. 1. Proposed flow diagram.

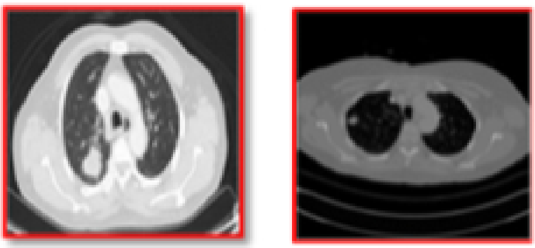

Fig. 2. LIDC-IBRI dataset Sample images.

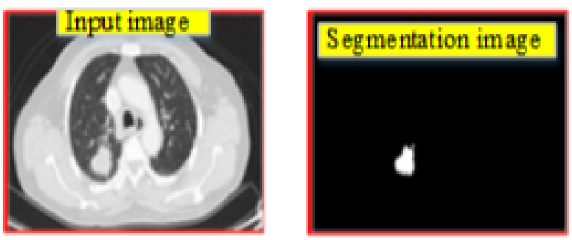

Fig. 3. Example Segmentation image.

2.2. Segmentation

LIDC-IDRI dataset image is read are clustered with the help of the FCM clustering algorithm. The Cluster images are segmented with the help of morphological operation. And some of the segmented images are shown in Fig. 3. The FCM clustering algorithm is defined in the below section.

2.2.1. *FCM Clustering Algorithms*

FCM is the most efficient data cluster algorithm. In this work, it plays a segmentation process. And, it's automatically determined for the number of clusters could enhance the detection accuracy. FCM was proposed by Dunn [18]. The standard partitioning the data of FCM objective function as $\{xk\}_{k=1}^{N}$ into c clusters is agreed as

$$J_{\mathrm{FCM}} = (U, V) = \sum_{i=0}^{c} \sum_{k=1}^{N} \mu_{ik}^{\rho} \mid\mid x_k - v_i \mid\mid^2 \tag{1}$$

Where V = $\{v_{i}{}_{(}i = 1)^c$ the prototype of cluster and array are U=μ_{ik} signifies the barrier matrix, c is the sum of cluster centroids, N is the sum of pixels or data points, x_k is the k^{th} pixel, and v_i is the centroid of i^{th} cluster. $\mid\mid x_k - v_i \mid\mid^2 = d_{ik} = d(x_k, v_i)$ is the distance extent among cluster middle v_i and the pixel x_k. This membership value fulfills the situations $\mu_{ik} \in [0, 1], 1 \leq i \geq c, 1 \leq k \geq N, 0 < \sum_{k=1}^{N} \mu_{ik} < N, 1 \leq i \geq c, and \sum_{i=1}^{c} \mu_{ik} = 1, 1 \leq k \geq N.$

Parameter p $\in (1, \infty)$ is a Weighing of exponent with every membership. It regulates the degree of blurriness of the ensuing organization and is typically set to 2. FCM's neutral task is lessened when pixels that are close to the center of gravity of the respective class are assigned high, and low membership standards are allotted when pixels are far from the center of gravity. The cluster focus is informed as

$$\mu_{ik} = \frac{1}{\sum_{j=1}^{c} (d_{ik}^2 / d_{jk}^2)^{1/p\prime}} \tag{2}$$

$$v_{ik} = \frac{\sum_{k=1}^{N} \mu_{ik}^{\rho} xk}{\sum_{k=1}^{N} \mu_{ik}^{\rho}} \tag{3}$$

2.3. Discrete Cosine Transform

DCT transforms an image signal from the spatial field to the frequency field.

$$D(i,j) = \frac{1}{\sqrt{2n}} c(i)c(j) \sum_{X=0}^{N-1} \sum_{y=0}^{N-1} p(x,y) \cos\left[\frac{(2x+1)i\pi}{2N}\right] \cos\left[\frac{(2y+1)j\pi}{2N}\right] \tag{4}$$

p(x,y) Is the x,y element of the copy denoted by the matrix p,N is the block that the DCT is done. The equivalence computes the one entry of $(i,j)^{th}$ converted image from the pixel value of the unique image matrix.

2.4. Meta-heuristic Bat Optimization Algorithm

Specific echolocation features of the microbats Meta-heuristic Bat optimization Algorithm has introduced in this study. Approximate or idealized rules of bat-inspired algorithms are defined in below.

1. All bats use echolocation to determine distance and magically "know" the variance among food/prey and ground barriers;

2. Bats fly randomly with velocity is denoted as v_i at position x_i with a stable frequency f_{min}, varying wavelength λ and loudness A_0 to search for prey.

3. Even though the volume can alter in several means, we accept that the volume varies from a large A0 to the lowest constant value of Amin.

Another evident generalization is that ray tracing is not used to estimate time delay and 3D topography. Although this can be a decent article for use in computational geometry, we won't use it because it is extra computationally intensive in multi-dimensional circumstances. The best optimization solution chosen was used as the n CNN learning rate. The bit code of the bat procedure is defined below.

Pseudocode of the bat procedure
Objective function f(y)=(y1,.....yd)^T
Put the bat population y_i (i=1,2,.....n) & v_i
Delineate the pulse frequency f($_i$)at y($_i$)
Put pulse rate r and the soundness of B_i
While(t < Maximum sum of iteration)
If (rand > r($_i$))
Choose solution between the best solutions
Generate a local solution around the chooses solution
end if
Produce new solution by flying randomly
If (rand < B_i & f(Y_i) < f(Y*))
Allow the novel solution
Upsurge r($_i$) and lessen B($_i$)
end if
Rank the bats and find (Y*) present best
end while
Previous process outcome and visualization

2.5. Convolutional Neural Network (CNN)

The CNN training is based on the back propagation algorithm [19] and uses the vector of the training pattern x with the associated target classes y as input. Learning is accomplished by comparing each CNN's output to the consistent desired goal, and their different results in a learning error. In mathematical terms, assuming the subsequent CNN cost function,

$$E(\omega) = \frac{1}{2}\sum_{p=1}^{p}\sum_{j=1}^{N_i}(O_{j,p}^1 - y_{j,p})^2 \tag{5}$$

Which is the variance among the desirable output $y_{j,p}$ for the input x_i and the CNN $o_{j,p}$ of j neuron that belongs to l layer, N_l. Our goal is the reducing of cost function E(ω), finding a minimizer $\tilde{\omega} = \tilde{\omega}^1, \tilde{\omega}^2, ..., \tilde{\omega}^v \in \mathbb{R}^v$,where $v = \sum_{(k=1)}^{L}$ WeightNum (k) and signify that the space of weight $\mathbb{R}^v$ is equal to the sum of weights (WeigtNum(.)) at each k layer of complete layers of the CNN network. The illustrious SGD (Stochastic gradient descent) optimization procedure uses the gradient error function,

$$\nabla E_i = (\frac{\partial E_i}{\partial \omega_i^1}, ..., \frac{\partial E_i}{\partial \omega_i^v}) \tag{6}$$

In each i training iteration, update the CNN weights according to the following formula to minimize the training error:

$$\omega_{i+1} = \omega_i - n\nabla E_i(\omega_i) \tag{7}$$

Where n signifies the learning rate (step) value. The n has been selected with the help of metaheuristic optimization techniques.

3. Result and discussion

In this unit, we deliberate the discussion of model outcomes with different parameters by using both proposed and some existing schemes. The Projected system is investigated using the tool such as, MATLAB with 3.0 GHz frequency Intel i3 processor, the hard disk memory capacity space is 1TB and 8 GB RAM. Also, defining the simulation outcome efficiency of the proposed system is compared with some recent traditional systems on the accessible datasets described in section 3. In this study, we compare two optimization techniques, such as ACO and PSO with the proposed method.

3.1. Evaluation Metrics

The assessment metrics are used to evaluate the segmentation efficiency and classification of our technique. For the segmentation, the valuation parameter includes sensitivity (SE), specificity (SP), F-Measure (FM) accuracy (AC), Recall (R), G-mean (GM) and Precision (P). The distinct presentation factors as:

$$R = \frac{tp}{tp + fn} \tag{8}$$

$$P = \frac{tp + tn}{tp + tn + fp + fn} \tag{9}$$

$$FM = \frac{2.R.P}{R + P} \tag{10}$$

$$SE = \frac{tp}{tp + fn} \tag{11}$$

$$SP = \frac{tn}{tn + fp} \tag{12}$$

$$AC = \frac{tp + tn}{tp + fp + tn + fn} \tag{13}$$

$$GM = \sqrt{tp_{rate}} \times tn_{rate} \tag{14}$$

Where, t_p,t_n f_p, and f_n represent the sum of cases such as a true positive, false negative, true negative, and false positive.

3.2. Qualitative analysis

The proposed system performance has certified in several conducts in this qualitative analysis. In the below section, we briefly discussed the analysis of the scheme. The sensitivity (SE), specificity (SP), F-Measure (FM), Recall (R), G-mean (GM), and Precision (P) comparative analysis is distinct in Table 1.

Table 1 presents the four classification techniques performance, such as using only CNN, CNN with PSO, CNN with ACO, and CNN with BAT algorithms, analyzed with three iterations such as 5, 10, and 20. These different kinds of methods and several iterations applied to determine the given parameter metrics. Each method has three iterations. Initially, only the CNN method attains the better outcome performance of iteration 5 in best precision value of 81.076 %, SP of 77.50 %, and FM of 74.69 %. In the combination of PSO with CNN, this scheme attained the highest SE value of 79.87 %, SP of 88.50 %, in 20^{th} iteration. It is better than the previous two iterations. This method attains better parameter metrics than the only CNN method. In another method of ACO with CNN method attain the better simulation outcome values such as SE of 100 %, SP of 93 %, recall of 100, in the 20^{th} iteration. This method performance is much better than the previously existing method of PSO with CNN. BAT with CNN method gets the performance value of SE 99.5 %, SP of 93.50 % in 10^{th} iteration. It was also better than previous methods outcomes. In another BAT-CNN method, attain better performance in the 20^{th} iteration. The highest value of SE of 99.37 %, SP of 95.50 %, the precision of 95.84 %, and recall value of 99.37 %. These two iterations attend the better performance the previously existing methods and values are highlighted in bold fonts. Table 1 below displays a qualitative analysis of the accuracy of different existing methods with our proposed method. Only CNN attained a better accuracy of 76.3 % in the 5th iteration. Finally, BAT with CNN method attains a better accuracy of 97.25 % and 97.43 % in iteration 20^{th}. However in 5^{th} and 10^{th} iteration attained the accuracy of 96.75 % and 96.50 %. It is lower than the 20^{th} iteration. The better accuracy value of the table is highlighted in bold.

3.3. Quantitative analysis

In this division, the proposed system has compared with various existing systems. The analyses have distinct in Fig. 4. It shows the accuracy of quantitative analysis with the proposed scheme with some existing scheme. In [7] used the CNN classifier method with the LIDC IDRI dataset to attain the 84.32 % accuracy. In another author [9] using the same dataset with SVM classifier to achieve 92 % accuracy. It is better than the CNN classifier method. But the author [8] achieves better accuracy of 97.14 % by using the LDA classifier scheme. But our proposed scheme by using the LIDC IDRI dataset to evaluate results by using three different classifiers such as PSO-CNN attain accuracy of 86.75, ACO-CNN attain 96.75 % and BAT-CNN attain 97.43 %.

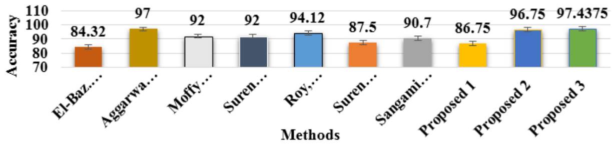

Fig. 4. Comparative analysis of the proposed system with various existing systems.

In proposed method presented three models achieved better accuracy than existing methods (See Fig.4). The proposed scheme is most useful for lung cancer prediction and detection. So we suggest this scheme is applicable for the medical sector to recover the lung cancer patient and reduce the real-world mortality rate.

4. Conclusion

This article shows that the PSO, ACO, and Bat algorithms develop the accuracy of CNN. Despite the upsurge in computation times, the projected scheme's error is less than the initial CNN for completely the changes of the time. The system CNN with the BAT optimization algorithm ensures that 97.43 % of accuracy with minimum classification error 2.57. The proposed analysis shows that the FCM based segmentation and CNN with the BAT classification technique are well suitable for the prediction and detection of LC. In the future, the projected model will be further optimized for the classification of pulmonary nodes. In addition, images will be classified according to the degree of cardiovascular disease of the lung nodules, which is important for LC treatment and detection in medical applications.

Table 1. Comparative analysis of the projected system.

Method	Iteration	SE	SP	P	R	FM	GM	ACC
Only CNN	5	75	77.5000	81.0760	75	74.6890	73.8051	76.2500
	10	83.7500	51	69.7130	83.7500	70.0178	49.2125	67.3750
	20	64.3750	75	- -	64.3750	- -	58.8374	69.6875
PSO_CNN	5	79	84.0000	81.3525	79	77.4461	78.7935	81.5000
	10	73.7500	84.2500	85.6903	73.7500	71.8823	73.8997	79.0000
	20	79.8750	88.5000	88.5084	79.8750	82.1984	82.9909	84.1875
ACO_CNN	5	99.5000	92	92.8509	99.5000	83.6714	95.9758	95.7500
	10	99.7500	93.7500	94.4620	99.7500	96.9375	96.6411	96.7500
	20	100	93	93.6371	100	96.6675	96.4065	96.5000
BAT_CNN	5	99.5000	94	94.5642	99.5000	96.8951	96.6658	96.7500
	10	99.5000	93.5000	94.1732	99.5000	96.6844	96.3932	96.5000
	20	99.3750	95.5000	95.8398	99.3750	97.5262	97.3886	97.4375

References

[1] Mahdi Mohammadian, Hamid Salehiniya, Azam Safari, Khadijah Allah Bakeshei, Fatemeh Allah Bakeshei, and Abdollah Mohammadian-Hafshejani. Disparity and trends in the incidence and mortality of lung cancer in the world. *Biomedical Research and Therapy*, 5(6):2348–2364, 2018.

[2] Robert Timmerman, Rebecca Paulus, James Galvin, Jeffrey Michalski, William Straube, Jeffrey Bradley, Achilles Fakiris, Andrea Bezjak, Gregory Videtic, David Johnstone, Jack Fowler, Elizabeth Gore, and Hak Choy. Stereotactic body radiation therapy for inoperable early stage lung cancer. *JAMA - Journal of the American Medical Association*, 303(11):1070–1076, 2010.

[3] Hosein Rafiemanesh, Mojtaba Mehtarpour, Farah Khani, Sayed Mohammadali Hesami, Reza Shamlou, Farhad Towhidi, Hamid Salehiniya, Behnam Reza Makhsosi, and Ali Moini. Epidemiology, incidence and mortality of lung cancer and their relationship with the development index in the world. *Journal of Thoracic Disease*, 8(6):1094–1102, 2016.

[4] Matteo Malvezzi, Cristina Bosetti, Tiziana Rosso, Paola Bertuccio, Liliane Chatenoud, Fabio Levi, Canzio Romano, Eva Negri, and Carlo La Vecchia. Lung cancer mortality in European men: Trends and predictions. *Lung Cancer*, 80(2):138–145, 2013.

[5] J Vansteenkiste, C Dooms, C. Mascaux, and K. Nackaerts. Screening and early-detection of lung cancer. *Annals of Oncology*, 23(SUPPL. 10), 2012.

[6] Alistair C. Lindsay, Arjun Nair, and Michael B. Rubens. Multidetector computed tomography of the aorta. In *Surgical Management of Aortic Pathology: Current Fundamentals for the Clinical Management of Aortic Disease*, pages 385–408. Springer International Publishing, jan 2019.

[7] Ayman El-Baz, Garth M. Beache, Georgy Gimel'Farb, Kenji Suzuki, Kazunori Okada, Ahmed Elnakib, Ahmed Soliman, and Behnoush Abdollahi. Computer-aided diagnosis systems for lung cancer: Challenges and methodologies, 2013.

[8] Taruna Aggarwal, Asna Furqan, and Kunal Kalra. Feature extraction and LDA based classification of lung nodules in chest CT scan images. In *2015 International Conference on Advances in Computing, Communications and Informatics, ICACCI 2015*, pages 1189–1193, 2015.

[9] Moffy Vas and Amita Dessai. Lung cancer detection system using lung CT image processing. In *2017 International Conference on Computing, Communication, Control and Automation, ICCUBEA 2017*, 2018.

[10] Suren Makaju, P. W.C. Prasad, Abeer Alsadoon, A. K. Singh, and A. Elchouemi. Lung Cancer Detection using CT Scan Images. In *Procedia Computer Science*, volume 125, pages 107–114, 2018.

[11] Tanushree Sinha Roy, Neeraj Sirohi, and Arti Patle. Classification of lung image and nodule detection using fuzzy inference system. In *International Conference on Computing, Communication and Automation, ICCCA 2015*, pages 1204–1207, 2015.

[12] A Asuntha, A Brindha, S Indirani, and Andy Srinivasan. Lung cancer detection using SVM algorithm and optimization techniques. *Journal of Chemical and Pharmaceutical Sciences*, 9(4):3198–3203, 2016.

[13] P. B. Sangamithraa and S. Govindaraju. Lung tumour detection and classification using EK-Mean clustering. In *Proceedings of the 2016 IEEE International Conference on Wireless Communications, Signal Processing and Networking, WiSPNET 2016*, pages 2201–2206, 2016.

[14] Frank E. Curtis and Katya Scheinberg. Optimization Methods for Supervised Machine Learning: From Linear Models to Deep Learning. In *The Operations Research Revolution*, pages 89–113. INFORMS, sep 2017.

[15] James Martens. Deep learning via Hessian-free optimization. In *ICML 2010 - Proceedings, 27th International Conference on Machine Learning*, pages 735–742, 2010.

[16] G. E. Hinton and R. R. Salakhutdinov. Reducing the dimensionality of data with neural networks. *Science*, 313(5786):504–507, jul 2006.

[17] Oriol Vinyals and Daniel Povey. Krylov subspace descent for deep learning. In *Journal of Machine Learning Research*, volume 22, pages 1261–1268, 2012.

[18] Xin She Yang. *Engineering Optimization: An Introduction with Metaheuristic Applications*. 2010.

[19] Srinath Balasubramanian, Arunapriya Panchanathan, C. Bharatiraja, Sanjeevikumar Padmanaban, and Zbigniew Leonowicz. Module based floorplanning methodology to satisfy voltage island and fixed outline constraints. *Electronics*, 7(11):325, nov 2018.